

Figure 1. Variation of speed in manual positioning

The assisted manual operation concept is present in several works found in literature, aiming to not fully automatize processes and keeping the decision making for the operator. As shown in Rosenberg (1993), the idea is to help the human operator to perform tasks, improving its performance, like the ruler helps the task of drawing a line, overlaying virtual fixtures to the user, like a virtual wall to restrict motion, for example. The results shows decreased time to perform tasks when appropriate virtual fixtures are used. In Abbott *et al.* (2007) different forms of interaction between human and the robotic device are presented. In special, when the device's kinetic is given by the operator and the control law uses the information of position and velocity to create the virtual fixtures, it can be classified as impedance type. For imposing the restrict motion of a stiff wall, active actuators tends to require larger power, fast response and still can occurs instability, imprecision and offers danger to the operator. Passive actuators, on the other way, only dissipates energy from the system and therefore can make a decreasing system's energy function and, by consequence, natural stability, being capable of sustaining a virtual barrier with good performance (An and Kwon, 2002). Other advantages are being more secure for direct operation by humans and, in the case of friction brakes, good relation between energy consumption and energy dissipation or anti-torque for its volume.

Overlaying virtual fixtures-like layers for teleoperation on machine tools is presented by Garcia and Horikawa (2007), letting the operator decides the tool path while machining, instead of a NC program, but filtering the commands to not allow the tool to advance in certain prohibited regions, which can be the final part's dimensions. The information given to the control software, as a perimeter or area, is more compact and fast to be written than a full machining NC procedure.

A mechanism typically used in manual machines converts torque, given by the operator, to linear motion, guided by a bus, thru screw and nut. One entirely spin on the maniple usually represents a linear displacement from 2 to 8mm, giving a very slow and smooth motion with considerable force amplification. Another important characteristic of this mechanism is the overhauling condition, which for a given helix angle and friction coefficient, can turn forces in the linear side into dissipative reactions in the rotational side, therefore avoiding forces in the linear side to induce motion in the rotational side, which gives the operator the possibility to exert high cut forces without kickbacks, making the manual operation secure and reliable. For this reason is common to employ trapezoidal threads with friction in despite of low friction alternatives like ball bearings on manual machines. The combination of overhauling condition with the presence of backlash decouples the stopping inertia reflection of the work table motion to the axis, which its stopping dynamics becomes a function of only its own inertial moment. Mechanisms for backlash elimination between screw-and-nut contact are avoided for manual operation mainly because it can increases the friction and the force required for operation. With the existence of backlash, the work table with linear motion, where the precision is measured, could have inertial characteristics when initially in motion and stopping the maniple. However, it is not a preoccupation in real machines hence the bus guide friction is relatively high and the work velocity range for manual operation is relatively low.

Endo *et al.* (2007) proposes the use of an electromagnetic friction brake in the axis of the manual machine's maniple for imposing virtual barriers for prohibited regions, therefore assisting the machining work thru limiting the positioning process. This approach takes benefits from additive design (no great modifications to the machine structure), simplicity of construction, low forces to overcome (human input) and, mainly, the high relation between rotatory and linear motion that potentially can minimize the actuator error where the displacement is measured. The results of this work showed a maximum standard deviation of 0.32mm, which for a normal distribution gives the final position within $\pm 0.64\text{mm}$ for 95% of reliability. Based on the norm NBR/ISO 2768 (2001), as reference of fulfillment, the standard toleration for pieces between 30 and 120mm is $\pm 0.15\text{mm}$ for fine works, which in a normal distribution requires a standard deviation of $\pm 0.075\text{mm}$ for 95% of reliability. Therefore, the final results itself didn't archive standard real world's requisites. This can be attributed to the low resolution encoder used, inefficient brake design and control algorithm. However, the concept still holds horizon for further studies.

There are several electromagnetic brakes available, like based on the friction of two surfaces, magnetorheological fluid or magnetic particles. The friction type has the inherit nonlinearities from friction phenomenon, but it has the best relation between counter-torque, volume, power needed to operate and simplicity of construction (Orthwein, 2004). The friction reaction force is the response of a tribological system between the bodies, which takes in count several factors like the materials, velocity, surface characteristics, temperature, presence of vibration, contaminants, constructive characteristics like alignment and parallelism that influences the pressure contact distribution, adsorbed gases on the surface, wear, oxide formation, etc (Blau, 1995). For this reason, the friction phenomena cannot be considered time invariant and the proposed system has to archive high immunity to friction variations, aiming to be archived with better mechanical design and electronic compensation. A new friction brake-based prototype was built to continue with the studies initialized by Endo *et al.* (2007), with the objective to statically evaluate the boundaries of unknown parameters and testing of control algorithms to improve the positioning precision to meet real world expectations.

2. THE NEW PROTOTYPE

Based on the prototype built by Endo *et al.* (2007), a new prototype was developed for studying the manual servo assisted positioning, with the objective to evaluate brake control algorithms. The brake itself was redesigned from the original and the ball bearing was eliminated. Trying to maximize the counter-torque, aiming to reduce the deceleration time and thus reduce the effects of uncertainties in the final position, the contact area and the coil's power was increased. The new prototype consists basically in the brake, a maniple and a rotatory encoder solidary to the same axis. The brake was built based on a commercial electromagnetic pulley clutch used in automotive air conditioning, chosen for the high torque, good built quality and easy access to parts. Also, a higher resolution encoder is used, with 10,000 counts per turn, giving, for a 6mm pitch thread, resolution of 0.6 μ m. The brake itself is a spring-return annular type (Orthwein, 2004), where one static disk magnetically attracts a rotor disk and the friction on the contact area generates the energy dissipation and counter-torque in the axis. As the contact area is the entire disc surface, its effects are maximized. The spring-return creates an air gap d , measuring about 0.2 to 0.4mm, giving zero friction when the brake is turned off, maintaining the original characteristics of the system for manual operation, and also helps to keep the pressure contact constant and less affected by misalignments. It was verified that the mass-spring behavior is overdamped, so no oscillation occurs. The schematic structure of the prototype can be viewed in Fig. 2.

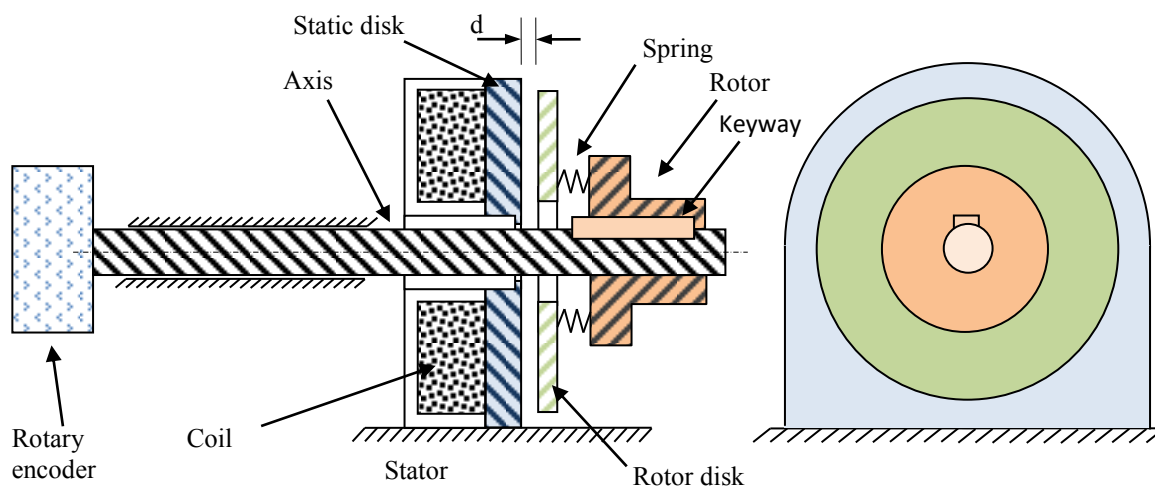


Figure 2. Slice view representation of the prototype, maniple omitted.

Given i the electric current applied on the brake's coil, a hysteresis of about 0.42A was identified between the coupling and decoupling of the discs, where de coupling occurs with about 0.71A and the decoupling with 0.29A. The measured inductance of the coil is $L=12.9\text{mH}$, its resistance $R=3.5\text{Ohms}$ and its nominal voltage operation $V=14\text{V}$, giving its maximum electric current $I_{max}=4\text{A}$. The graph of the hysteresis is presented in Fig. 3, where the current was increased slowly, thus making system's time delay negligible, to identify the hysteresis in electric current. With another experiment, exciting the brake with unity degrees inputs, the medium time delay to the disc coupling $t_d = 20\text{ms}$ was identified.

V. Sverzuti, O. Horikawa
Electromagnetic brake assisted positioning system – investigating control law for new prototype

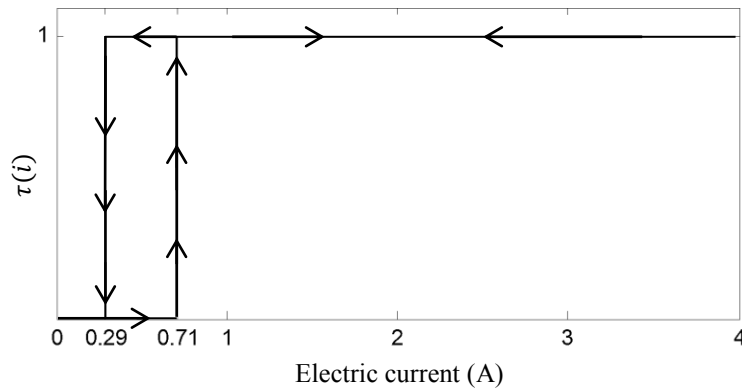


Figure 3. Hysteresis graph of surfaces contact.

2.1 Simplified model

As, in the process of machining, the motion is smooth and the operator tries to keep it constant, is assumed that the rate of change of the rotational speed is far lower than the control action's time to stops the motion. Therefore, it can be assumed that the system moves initially with constant velocity $\dot{\theta}_0 > 0$ in direction to the barrier which the limit is the desired position θ_d . The control action, as a passive actuator, is unidirectional and is only capable of lowering the system's velocity $\dot{\theta}$. Considering rigid bodies dynamic, the reactions on the axis can be represented by Eq. (1), where J is the moment of inertia, $\ddot{\theta}$ the angular acceleration, T_f the counter-torque generated by the brake and ε the sum of perturbations and non-modeled factors. In Eq. 2 is expressed the contact between the surfaces of the brake, with the dynamic contact function $\tau(i)$, and the discontinuity on the change from run to stop state, where is assumed that T_f will be greater than any perturbation when the velocity is zero, letting the system remains stable on that state. This assumption is considered realistic one time that 1) the coefficient of static friction is bigger than the dynamic one; 2) the objective is to stop motion and remains stable, so full power can be applied to the actuator one time the system has stopped. The computation model can thus be simplified and the velocity integrator can saturates at level zero, avoiding problems with computational imprecision.

$$J \cdot \ddot{\theta} = T_f + \varepsilon \quad (1)$$

$$T_f(i, \dot{\theta}, \varepsilon) = \begin{cases} -\tau(i) \cdot K \cdot i, & \text{if } \dot{\theta} > 0 \\ -\tau(i) \cdot \varepsilon, & \text{if } \dot{\theta} \leq 0 \end{cases} \quad (2)$$

The $\tau(i)$ contact function incorporates the hysteresis and a fixed deadtime $t_d = 20\text{ms}$, returning zero when there is gap and 1 when there is contact between surfaces, therefore emulating the time for nulling the gap and coupling the friction surfaces, as identified in the prototype. In the K function is represented the relation between current applied and counter-torque, which in principle is a stochastic parameter, possibly velocity dependent and variant in time, as it involves the friction phenomena, as seen on Blau (1995). Nevertheless, for the scope of this paper, K is assumed to be constant in the simulations and its non-modeled effects would be interpreted as perturbations on ε .

Neglecting the back-emf of the rotor moving towards the stator while it nulls the gap, the electric current can be given with the transfer function of a first order LR series circuit, where the voltage V is the input, showed on Eq. 3. The actuator input $V(t)$ is referenced as the control input $u(t)$ on the control laws that will be presented.

$$\frac{I(s)}{V(s)} = \frac{1}{R + L \cdot s} = G_{coil} \quad (3)$$

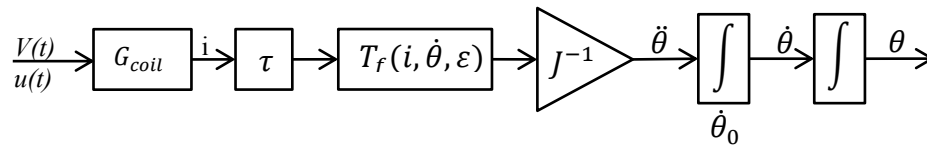


Figure 4. Block diagram of the simplified model used in the simulations.

2.2 The control problem

Mainly, the control problem is to archive performance within the precision range, as stability will occur due to the passive actuation. Given the current velocity $\dot{\theta}$, that can be estimated by differentiation of the position encoder, and the current position θ , a control law $u(t)$ must be designed to bring the system to zero velocity at a given position θ_d . The control approach used in the previous work by Endo *et al.* (2007), proportional feedback with feedforward (f.f.) term, is reviewed and criticized, so a new and simpler approach is presented, based on the ON/OFF control with f.f. term.

2.2.1 Proportional with feedforward control

The control algorithm used by Endo *et al.* (2007) can be viewed as a feedback control, proportional to the positioning error, with a f.f. component for dealing with the unidirectional actuator. Without the f.f. portion, the position would violate the setpoint of the virtual barrier to the actuator acts proportionally to the error, in other words, the control would act only for a violated position. The f.f. term, represented by M in the final control law shown in Eq. (4), makes the control output to act before the desired position, as illustrated in Fig. 5 (a). It was presented in the work that, for implementation simplicity, control action was discretized to 50%, 75% and 100% of the actuator's full power for equivalent error ranges. The criticism to this approach is that the control being proportional to the position error does not necessary brings the system to the desired position as, for the unilateral control, the final position is determined by the history of decrease in velocity, not in the position error itself. Another consideration is that the proportional control acts slower in relation to the application of full power to the brake, thus braking in greater time and giving more opportunity for final position drift due to disturbances, one time that the control law do not act to compensate them. This can be attenuated with high gains, until the point that for very high values of the proportional gain, the controller acts almost like an ON/OFF control.

$$u = K_p e + M \Rightarrow J \cdot \ddot{e} - K_p e - M = 0 \quad (4)$$

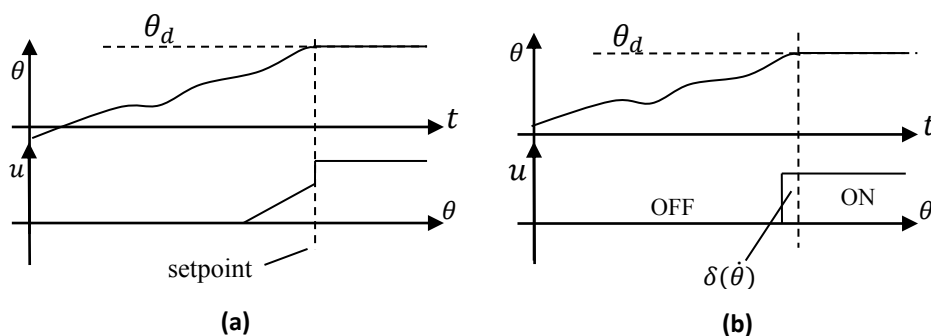


Figure 5. (a) Proportional control with feedforward; (b) ON/OFF control with feedforward.

2.2.2 ON/OFF with feedforward control

A simpler and fast approach is proposed using ON/OFF control with a f.f. term to anticipate the actuator action. The ON/OFF control consists in switching the actuator ON, with full power, at the desired position. Based on Eq. (5), from the work-kinetic energy theorem, consider the following: 1) the range of possible velocity is restricted and reasonable small; 2) the friction dynamics is unknown, velocity dependent, possible time variant and difficult to model, but the variations should be statically bounded to an interval of confidence around a mean value; 3) the friction uncertainties, reflected on T_f , will be less expressive in the absolute final position error as higher the central value of T_f is. In other words, a high-counter torque brake gives fewer margins to friction errors.

V. Sverzuti, O. Horikawa
Electromagnetic brake assisted positioning system – investigating control law for new prototype

$$\Delta\theta = \frac{J}{2 \cdot T_f} \dot{\theta}_0^2 \quad (5)$$

Neglecting the nonlinearities of the actuator, the f.f. term would be proportional to the square of the initial velocity. But the main drift in final position is expected to be caused by the actuator's deadtime t_e , due mainly to the air gap and the delay to build sufficient electric current due to the coil's inductance, resulting in the f.f. term of Eq. (6). Equation (7) shows the ON/OFF control rule with the f.f. term. The control action is illustrated in Figure 5 (b).

$$\delta = \dot{\theta} \cdot t_e + K_d \cdot \dot{\theta}^2 \quad (6)$$

$$u = \begin{cases} ON, & \text{if } \delta \geq \theta_d - \theta \\ OFF, & \text{otherwise} \end{cases} \quad (7)$$

3. METODOLOGY

The positioning variable controlled in the prototype is the angular position of the axis, but for reference purposes is considered that the axis is coupled to a nut-screw mechanism with pitch=6mm and the results will be displayed in millimeters. It will be evaluated, by simulation, the proposed ON/OFF control algorithm with f.f. and an ON/OFF without f.f., which is simulated first to identify the f.f. terms. The speed range of the simulation is 6, 12, 18, 24, 30, 36, 42, 48, 54 and 60 rpm, considered equivalent to 0.6, 1.2, 1.8, 2.4, 3.0, 3.6, 4.2, 4.8, 5.4 and 6.0 mm/s in the linear side, respectively. To evaluate real implementation scenarios, where the simplicity is desirable, the f.f. term will be evaluated in two forms: 1) $\delta_1 = \dot{\theta} \cdot t_e$, assuming that the counter-torque is high enough to make the dissipation energy time neglected, so the f.f. compensation is for the deadtime; 2) $\delta_2 = a \cdot \dot{\theta} + b \cdot \dot{\theta}^2$ that is expected to be a better compensation with the second order term, but with a bigger computational cost. The parameters used in the simulations are given at Tab. 1 and was identified in the prototype, with exception for J and K that were estimated. In each simulation, given the initial speed $\dot{\theta}_0$ and position zero, the control setpoint for the virtual barrier is given by 0,3mm ahead, for the nominal pitch considered. Once identified the parameters of δ_1 and δ_2 , the two algorithms are simulated within the same velocity range. Finally, it is simulated δ_1 with 20% variation in t_e , giving 1% increments, to evaluate its sensibility on imprecise parameter's identification, variation with time or nonlinearity that can occurs in real implementations.

Table 1. Parameters used in the simulation

$J = 0.02 \text{ kg} \cdot \text{m}$	$K = 15 \text{ N} \cdot \text{m/A}$
$\dot{\theta}_0 = 180 \text{ deg/seg}$	$H_{i+} = 0.7 \text{ A}$
$L = 13 \text{ mH}$	$H_{i-} = 0.3 \text{ A}$
$R = 3.5 \Omega$	$V_{\text{sat}} = 14 \text{ Volts}$
$\theta_d = 360^\circ$	$\text{Pitch} = 6\text{mm}$

To evaluate the control algorithm's performance, the main variables considered are the absolute maximum final positioning error and its standard deviation (σ). As reference is adopted the fine tolerances of the norm NBR/ISO 2768 (2001), giving a maximum absolute error of 150um and σ of 75um. A relation between the reference values is made with the obtained absolute final error, representing the limit of the friction relative influence on T_f , considering that the other parameters are well known. This can also be seen as a rejection rate of relative friction disturbances of the control algorithm.

4. RESULTS

Figure 6 (a), (b) and (c) shows the position vs velocity plot, where can be seen the expressive improvement in the final position dispersion with the added f.f. term. Based on the error data resulting of the ON control simulation, the coefficients of the two f.f. terms was identified, resulting in $t_e = 20.73 \text{ lms}$, $a = 20.600 \cdot 10^{-3}$ and $b = 167.4 \cdot 10^{-6}$. The anticipated action inserted by the f.f. term δ_n is represented in (b) and (c) by the diagonal line, as when the line intersects with the velocity vs position curve, the actuator is turned on. The velocity vs maximum absolute error for the two f.f. approaches can be seen on (d). Figure 7 shows the maximum absolute error and standard deviation to a range of

percentage dispersion around t_e , with the δ_1 control algorithm. Table 2 shows the final simulation results and the deceleration time, which is equal to all algorithms as the control action is the same, but executed at different positions.

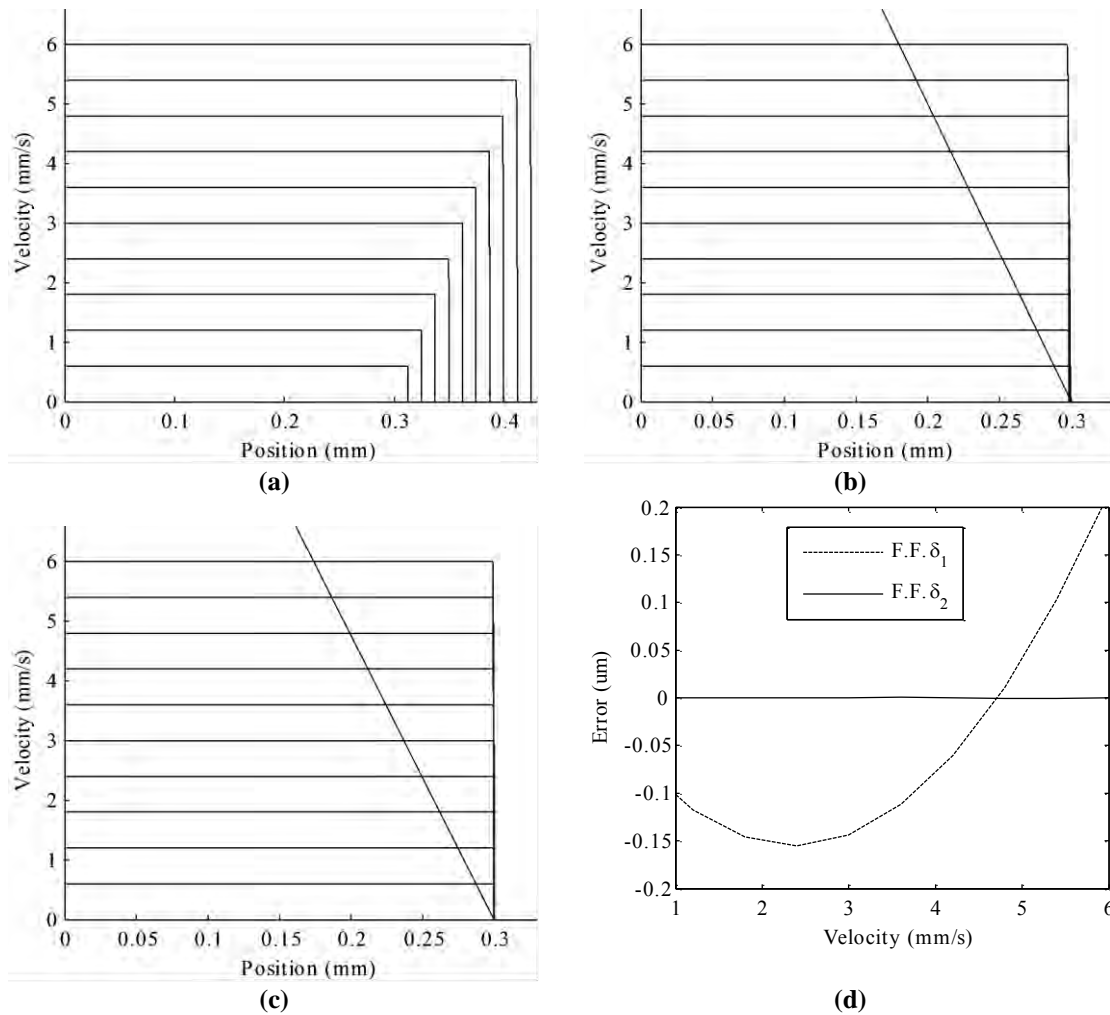


Figure 6. Results of the simulations with desired final position equal to 0,3mm for (a) the ON/OFF approach; (b) ON/OFF with feedforward δ_1 term; (c) ON/OFF with feedforward δ_2 term; (d) comparison of error between the first degree δ_1 and the second degree δ_2 feedforward terms.

Table 2. Simulation results.

Axis Velocity (rpm)	Error (um)			Deceleration time (us)
	ON/OFF	ON/OFF with f.f. δ_1	ON/OFF with f.f. δ_2	
6.0	12.370	-0.069	< 1nm	33
12.0	24.760	-0.118	< 1nm	67
18.0	37.170	-0.146	< 1nm	100
24.0	49.600	-0.155	< 1nm	134
30.0	62.050	-0.144	< 1nm	167
36.0	74.520	-0.112	< 1nm	201
42.0	87.011	-0.060	< 1nm	234
48.0	99.522	0.011	< 1nm	267
54.0	112.051	0.103	< 1nm	301
60.0	124.603	0.215	< 1nm	334
Mean	68.366	-0.048	< 1nm	

V. Sverzuti, O. Horikawa
Electromagnetic brake assisted positioning system – investigating control law for new prototype

Standard Deviation (σ)	37.756	0.122	< 1nm
Abs. max. error	124.603	0.215	< 1nm
Relative σ	2.0	614.8	> 75,000
Relative max. abs. error	1.2	697.7	> 150,000

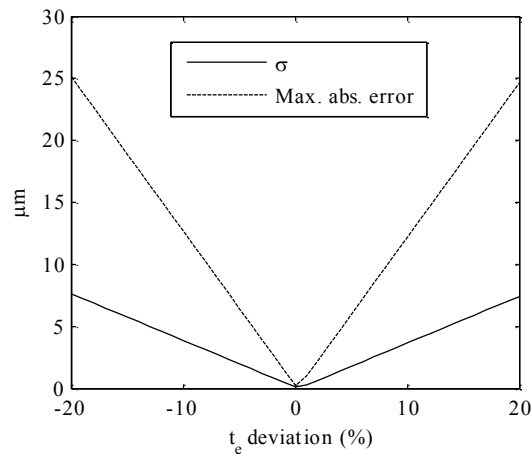


Figure 7. Sensibility of the maximum absolute error and standart deviation to $\pm 20\%$ variation in t_e .

5. CONCLUSIONS

The result of the simulations shows that the ON/OFF control without a f.f. compensation has a nearly 1:1 friction relative variation rejection. This means, for say, that 20% variation on T_f or deceleration time caused by friction would drifts the final positions, in the worst case considered, by nearly 20%. Therefore, the ON/OFF control itself has great chances to be inaccurate in real applications. With the added f.f. δ_1 term, however, the rejection is large, which proves that, for certain circumstances, the braking dynamic can be omitted. An optimal performance is seen with the term δ_2 , as it has the same degree of the model, and is expected to perform better than δ_1 in real world implementations, but this still have to be evaluated with the real prototype, as it is also expected imprecise parameter's identification or nonlinearities. This sensibility to the variation of the coefficient of δ_1 is verified on Fig. 7 to be linear and considered high, as it decreases the friction rejection in the abs. maximum error from 698 to approximately 30 with only 10% in variation in t_e and from 615 to approximately 5 in the sigma rejection, which can justify the development of an adaptation rule for the f.f. coefficients to try to minimize the error. The results shown are promising about the viability of precision positioning with passive actuator and further experimental investigation are needed to verify if the final results will be bounded to the precision requirements.

6. ACKNOWLEDGEMENTS

This project was conducted under grant from "Fundação para o Desenvolvimento Tecnológico da Engenharia - FDTE" (SP, BRAZIL).

7. REFERENCES

- Abbott, J. J., Marayong, P., Okamura, A. M., 2005. "Haptic Virtual Fixtures for Robot-Assisted Manipulation", In *12th International Symposium of Robotics Research (ISRR)*.
- An, J., Kwon, D.S., 2002. "Haptic Experimentation on a Hybrid active/Passive Force Feedback Device", In *Proceedings of the 2002 IEEE International Conference on Robotics & Automation*, Washington DC.
- Blau, P. J., 1995. *Fiction science and technology*, Marcel Dekker Inc, New York.
- Endo, R., Garcia, L. N. F., Horikawa, O., Utida, F. T., 2007. "Simple Architecture for a manual and servo assisted hybrid system for position control in machine tools", In *Proceedings of 19th International Congress of Mechanical Engineering – COBEM2007*. Brasília, DF, Brazil.

22nd International Congress of Mechanical Engineering (COBEM 2013)
November 3-7, 2013, Ribeirão Preto, SP, Brazil

- Garcia, L. N. F., Horikawa, O., 2007. "Manual and servo assisted hybrid system for position control in machine tools",
In *Proceedings of 19th International Congress of Mechanical Engineering - COBEM2007*. Brasília, DF, Brazil.
- NBR/ISO 2768, 2001. *Tolerâncias gerais – Parte 1: Tolerâncias para dimensões lineares e angulares sem indicação de tolerância individual*. Equivalent to ISO 2768-1:1989. ABNT – Associação Brasileira de Normas Técnicas, Brazil.
- Orthwein, W. C., 2004. *Clutches and Brakes Design and Selection*, 2nd ed, Marcel Dekker Inc.
- Rosenberg, L. B., 1993. "Virtual Fixtures: Perceptual Tools for Telerobotic Manipulation". In *IEEE Virtual Reality Annual International Symposium*, Seattle, WA, USA. 18-22 Sep.

8. RESPONSIBILITY NOTICE

The authors are the only responsible for the printed material included in this paper.